Available on CMS information server **CMS CR 2006/023**

CMS Conference Report

3 May 2006

Impact of CMS Silicon Tracker Misalignment on Track and Vertex Reconstruction

N. De Filippis[1)]

L. Barbone[1)],O. Buchmueller[2)], F.P. Schilling[2)], T. Speer[3)], P. Vanlaer[4)]

CMS collaboration

Abstract

The alignment uncertainties of the CMS Tracker detector, made of a huge amount of independent silicon sensors with an excellent position resolution, affect the performances of the track reconstruction, the track parameters measurement and the vertex reconstruction. In order to study the impact of the mis-alignment of the CMS tracking devices on the previous procedures, realistic estimates for the expected displacements of the tracking systems are supplied in two different scenarios, the first supposed to reproduce the mis-alignment conditions during the first data taking while the second one related to long term data taking condition. Results about the track reconstruction are expressed in terms of the resolution on track parameters, the global efficiency of the track reconstruction and the fake rate in the two scenarios of mis-alignment, by comparing them with the scenario of a perfect alignment of the tracking devices. Primary vertex finding efficiency and position resolution are affected by the tracker mis-alignment, too.

Presented at *Workshop on Tracking In high Multiplicity Environments*, Zurich, October 03-07, 2005

[1)] Dipartimento Interateneo di Fisica dell'Universitá e del Politecnico di Bari e INFN Sezione di Bari, Bari, Italy

[2)] CERN, Geneva, Switzerland

[3)] Physik-Institut, Universitat Zuerich, Zuerich, Switzerland

[4)] Interuniversity Institute for High Energies (IIHE), Universite Libre de Bruxelles, Brussels, Belgium

1 Tracker misalignment

The silicon tracker detector of the CMS detector [1] is made of an inner silicon pixel detector and a silicon microstrip tracker. The pixel detector consists of three cylindrical layers in the barrel at radii 4.4, 7.5 and 10.2 cm (TPB), and two pairs of end-cap disks at $|z| = 34.5$ cm and 46.5 cm down to a pseudo rapidity η of $|2.2|$ (TPE). The hit position resolution is $\sim 10\,\mu\mathrm{m}$ in the (r-ϕ) plane and 17 $\mu\mathrm{m}$ in (r,z) plane. The silicon microstrip detector covers radii between 20 and 110 cm. The barrel region is divided into an Inner Barrel (TIB), made of four layers of sensors, and an Outer Barrel (TOB) made of six layers. The TIB is completed on each side by three inner disks (TID). The forward region is equipped with nine end-cap disks (TEC) [3]. The hit position resolution achieved is $\sigma_{r,\phi} = 40 - 60\,\mu\mathrm{m}$ in (r-ϕ) plane and 500 $\mu\mathrm{m}$ along z.

Unavoidable uncertainties on the exact positions of the silicon sensors in the tracker exist due to the mechanical accuracy to position the individual silicon modules within each of the subdetectors (TIB, TOB, and TECs), which is about $50\,\mu\mathrm{m}$, and to the mechanical accuracy between the subdetectors which will more likely be of the order of mm.

The detector positional accuracy, estimated from Monte Carlo Simulation, needed to start the pattern recognition in the CMS silicon tracker has to be about $100\,\mu\mathrm{m}$. Alignment procedures are implemented with the purpose to determine the absolute position of a sufficient number of mechanical support structure elements with a precision better than $100\,\mu\mathrm{m}$. This alignment will be performed with the optical laser. A sufficient statistics of reconstructed tracks will be used to determine the positions of the detectors with an accuracy of 10 $\mu\mathrm{m}$ (in order to reconstruct the track parameters with the best resolution).

Realistic displacements for the individual detector elements are provided as input to a dedicated software in order to simulate the tracker misalignment and to derive the misalignment effects on the reconstruction. The misalignment of the CMS tracker is introduced:

- by displacing the detector modules which host the reconstructed hits while leaving the local hits in place (so no need to generate events with a distorted geometry);
- at various hierarchical levels, like for example at the level of misplacing the whole forward end-cap or just one rod or detector module in the outer barrel. Possible displacements implemented are rotations around x, y, z and shifts in x, y, z directions.

Two general misalignment scenarios are studied:

- the *First Data Taking* scenario that is supposed to resemble the misalignment conditions during the first data taking, after collecting an integrated data luminosity of $< 1\,\mathrm{fb}^{-1}$; the mechanical uncertainties and the laser alignment are expected to reduce the alignment uncertainties at a level of 100 μm for each module.
- the *Long Term* scenario that will address the impact of the alignment uncertainties on the tracking performance, with an integrated data luminosity of few fb^{-1}. A factor 10 of improvement in the alignment uncertainty with respect to the previous scenario is expected to be reached due to the large number of tracks that will allow to carry out a complete track-based alignment down to the sensor level, resulting in an overall alignment uncertainty close to the tracker intrinsic position resolution.

Both in the two scenarios all the modules in the tracker are randomly moved according to their mounting precision. Also the ladders in the pixel barrels, the rods in the inner and outer barrels, the blades in the pixel endcaps, the rings in the inner disks and the petals in the endcaps are randomly moved according to their mounting precision. All these random movements are applied in x, y and z direction.

For the much complex structures of the barrel layers and the endcap disks a shift in x, y and z direction is also used. Additionally the barrel layers and endcap disks are rotated around the z axis by a fixed amount. The fixed shifts and rotations are evaluated by profiting from the information about the misalignment of these tracker parts given by the laser alignment system, as detailed in Ref. [2]. The resulting values are used as input to a random number generator and the output of the random generator is used as the fixed shift or rotation of the layer or disk.

The mounting precisions of modules and substructures like ladders, rods, rings and petals, as expected in the *First Data Taking* scenario, are detailed in Table 1. Table 2 lists the expected values of the alignment uncertainties for layers (barrel) and disks (endcaps) after the laser alignment is performed, in the *First Data Taking* scenario.

	TPB [μm]	TIB [μm]	TOB [μm]	TPE [μm]	TID [μm]	TEC [μm]
Modules	13	200	100	2.5	105	50
Ladders/Rods/Rings/Petals	5	200	100	5	300	100

Table 1: Mounting precisions used for the *First Data Taking* Scenario (TPB and TPE already aligned with tracks).

	ΔX [μm]	ΔY [μm]	ΔZ [μm]	$\mathrm{R_z}$ [μrad]	LAS available
TPB	10	10	10	10	no
TIB	105	105	500	90	yes
TOB	67	67	500	59	yes
TPE	5	5	5	5	no
TID	400	400	400	100	no
TEC	57	57	500	46	yes

Table 2: Expected RMS values for shifts, ΔX, ΔY, ΔZ and rotation around z, $\mathrm{R_z}$, for rods, ladders, rings and petals after laser alignment (LAS), in the *First Data Taking* scenario.

2 Impact of misalignment on track reconstruction

The investigation of the effect of the misalignment of the CMS tracking devices on general track properties is performed using tracks of muons with a given transverse momentum, $\mathrm{p_T}$, or in a fixed range of $\mathrm{p_T}$ with or without pileup events at low luminosity ($\mathrm{L} = 2 \times 10^{33} \mathrm{cm}^{-2} \mathrm{s}^{-1}$).

Track reconstruction is performed in several steps according to the Kalman Filter formalism [4]; it includes the track seeding, the trajectory building, the ambiguity resolution and the smoothing of tracks. The error on the hit position in the track fit (called the Alignment Position Error) is obtained by combining the spatial resolution of the device with the alignment uncertainty estimated in the two misalignment scenarios. Reconstructed tracks are matched with the simulated if they share 50% of hits. All track candidates are classified as good tracks if they are reconstructed with at least eight hits (out of 17 only in the tracker detector).

The main effect of the tracker misalignment is observed in the resolution on the five track parameters $\mathrm{p_T}$, ϕ, $\mathrm{cot}\theta$, $\mathrm{d_0}$ and $\mathrm{z_0}$, defined at the point of closest approach of the track to the beam axis (this point is called the impact point); hence, $\mathrm{d_0}$ and $\mathrm{z_0}$ measure the coordinate of the impact point in the transverse and longitudinal plane ($\mathrm{d_0} = y_0 * \cos\phi - x_0 * \sin\phi$, where x_0 and y_0 are the transverse coordinates of the impact point). ϕ is the azimuthal angle of the momentum vector of the track at the impact point and θ the polar angle.

In Fig. 1 the dependence of the $\mathrm{p_T}$ resolution on the pseudo-rapidity η is reported as obtained with single muons with $\mathrm{p_T} = 100\,\mathrm{GeV}/c$. The $\mathrm{p_T}$ resolution is around 3% up to a pseudo-rapidity of $|\eta| = 1.75$ for a perfect tracker geometry. In the *First data taking* scenario the resolution is degraded to 6% in the same range of η; for higher values of $|\eta|$ the lever arm of the measurement is reduced so the resolution is degraded.

The mean shift and the σ of the gaussian fit of the residual distributions of the track parameters are reported in Table 3 for the different scenarios.

Single μ with $p_T = 100\,\mathrm{GeV}/c$.					
	p_T [GeV/c]	ϕ [rad]	$cot\theta$	z_0 [μm]	d_0 [μm]
Perfect tracker alignment					
Bias	-1.4	1.3×10^{-5}	1.4×10^{-6}	-0.2	-0.6
σ	2.1	1.0×10^{-4}	4.4×10^{-4}	34.4	9.4
Short-term tracker alignment					
Bias	-1.2	-2.2×10^{-6}	1.3×10^{-4}	-5.0	2.5
σ	6.8	5.0×10^{-4}	8.1×10^{-4}	69.0	34.8
Long-term tracker alignment					
Bias	-1.5	4.0×10^{-6}	-2.3×10^{-5}	6.6	2.3
σ	2.9	1.6×10^{-4}	6.4×10^{-4}	59.6	22.0

Table 3: Bias and resolution on track parameters for single muons with $p_T = 100\,\mathrm{GeV}/c$.

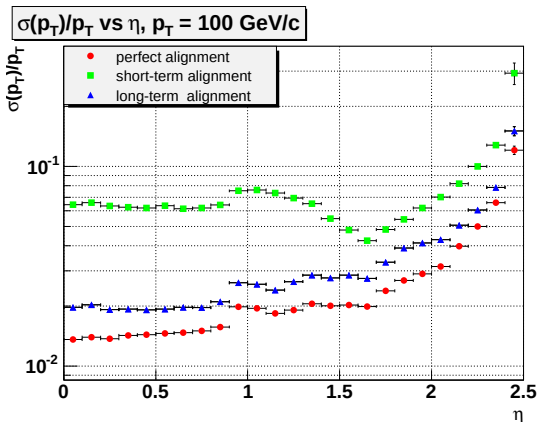

Figure 1: Transverse momentum resolution as a function of p_T for single muons with $p_T = 100\,\mathrm{GeV}/c$ in the scenario of perfect alignment, *first* and *long term data taking*.

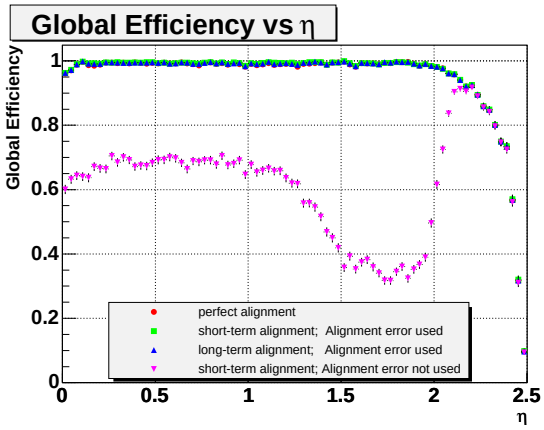

Figure 2: "Global efficiency" as a function of η for single muons with $p_T = 100\,\mathrm{GeV}/c$ in the scenario of perfect alignment and misalignment scenarios if the alignment uncertainties are taken into account in the definition of the Alignment Position Error (top markers) or just the detector resolution (bottom markers).

The "global efficiency" of track reconstruction which includes the efficiency of the algorithm, the acceptance, the hit efficiency and any other factor influencing reconstruction, is shown in Fig. 2 as a function of η, for the different scenarios. If the alignment uncertainties are not taken into account in the estimate of the error on the hit position during the track fit, the efficiency is strongly affected by the misalignment of the tracking device in the *First data taking* scenario, especially in the region of η between 1.5 and 2 where TID sensors with the largest misalignment and pixel detectors are used to reconstruct tracks (bottom markers in Fig. 2). The efficiency is fully recovered when accounting for alignment uncertainties in the track fit. This, however, causes an increase of the fake rate up to 10% in the same η region (with respect to 3.5% derived if the alignment uncertainties are not taken into account) because more compatible hits are found along tracks; a conservative estimate of the fake rate was obtained by using a sample of events $t\bar{t}H \rightarrow 8$ jets + X with pileup at low luminosity with a track multiplicity between 50 and 100 tracks per event.

3 Impact of misalignment on vertex reconstruction

Primary vertex reconstruction [3] starts with all the reconstructed tracks of the event and proceeds in the following steps:

- an initial track selection is performed to reject secondary tracks. The significance of the transverse impact parameter of track $\mathrm{d_0}/\sigma(\mathrm{d_0})$ is required to be smaller than 3 and the track $\mathrm{p_T}$ has to be larger than $1.5\,\mathrm{GeV/c}$;
- tracks are extrapolated to the beam line ($\mathrm{x} = 0$ and $\mathrm{y} = 0$) and grouped according to their separation in z, in order to form primary vertex candidates;
- each primary vertex candidate is then fit, and tracks incompatible with the vertex are discarded recursively, starting from the track with worst compatibility;
- a final cleaning of the vertex candidates is made. Vertices with a χ^2_{fit} probability below 1% are rejected. Vertices compatible with the beam line ($\mathrm{x} = 0$ and $\mathrm{y} = 0$) to less than 1% are rejected. The compatibility with the beam axis is computed accounting for a Gaussian beam spot with a width of $15\,\mu\mathrm{m}$ in x and y.

The performance of the procedure is defined mainly in terms of the vertex finding efficiency ϵ, defined as the efficiency to find any of the primary vertex candidates within $\Delta\mathrm{z} = 500\,\mu\mathrm{m}$ from the simulated signal vertex, and the position resolutions $\sigma_{\mathrm{x,y,z}}$, defined here as the standard deviation of a Gaussian fit to the distributions of the residuals with respect to the simulated vertex position in three dimensions, for the primary vertex candidate nearest to the simulated signal vertex.

The effect of tracker misalignment on primary vertex finding is investigated for three physics channels with very different kinematics at the primary vertex: $B_s^0 \rightarrow J/\psi\phi$ decays, $t\bar{t}H$ events, and Drell-Yan (DY) processes to $\mu^+\mu^-$ with $\sqrt{s} = 115\,\mathrm{GeV/c}$. The samples are simulated with low luminosity pile-up.

The vertex finding efficiency and the average multiplicities of reconstructed tracks from the signal primary vertex (after the algorithm selection cut on $\mathrm{p_T}$ above $1.5\,\mathrm{GeV/c}$) are given in Table 4. The primary vertex in the $B_s^0 \rightarrow J/\psi\phi$ sample is soft, with 12.4 reconstructed tracks per vertex (4.4 with a $\mathrm{p_T}$ above $1.5\,\mathrm{GeV/c}$). The $t\bar{t}H$ and DY events are harder and have larger track multiplicities.

	ϵ	Multiplicity of rec. tracks
Perfect tracker alignment		
$B_s^0 \rightarrow J/\psi\phi$	0.835 ± 0.005	4.4
$t\bar{t}H$	0.993 ± 0.001	20
DY	0.940 ± 0.004	9.4
Short-term tracker alignment		
$B_s^0 \rightarrow J/\psi\phi$	0.825 ± 0.005	4.6
$t\bar{t}H$	0.958 ± 0.003	19
DY	0.914 ± 0.004	9.4
Long-term tracker alignment		
$B_s^0 \rightarrow J/\psi\phi$	0.826 ± 0.005	4.4
$t\bar{t}H$	0.960 ± 0.004	20
DY	0.916 ± 0.004	9.4

Table 4: Primary vertex finding efficiency ϵ, multiplicities of reconstructed tracks from the signal primary with $p_T > 1.5$ GeV/c.

The effect of tracker misalignment on primary vertex finding efficiency is small with a maximum degradation of 3.5% observed among the samples studied. The reason for this drop is the larger fraction of vertices failing the selection cut on the compatibility with the beam line. The drop is identical in *short term* and *Long term* scenarios because the effect of misalignment on primary vertex finding is pixel-dominated. No differences are expected in the alignment uncertainties on pixel detectors in the two scenarios studied because the track statistic collected in an integrated data luminosity $< 1\ fb^{-1}$ is sufficient to align the pixel detector up to the intrinsic position resolution.

The resolutions, fraction of tails and biases are detailed in Table 5 for X and Y coordinates. In the *Long Term* misalignment scenario, the primary vertex biases in the three coordinates are consistent with the alignment shifts of the pixel barrel layers given as input for the simulation. In the short-term scenario, the misalignment of the silicon strip tracker is ten times worse, which further affects the primary vertex bias. The effect is larger for harder events, since the constraint on high-momentum tracks from hits in the silicon strip tracker is stronger (less multiple scattering).

The position resolution is significantly affected by the tracker misalignment. The degradation of the primary vertex resolution is of the same order of magnitude for soft and hard events (6-8 $\mu\mathrm{m}$ in absolute value). Thus, misalignments effects do not add up in quadrature with the resolutions obtained in the perfect alignment case because they come from different systematic shifts of different detector parts, giving rise to different track populations.

4 Conclusions

The effects of tracker misalignment in the *First Data taking* and in the *Long Term* misalignment scenarios are evaluated.

In the *First Data Taking* scenario the $\mathrm{p_T}$ resolution of single muons at $\mathrm{p_T} = 100\,\mathrm{GeV/c}$ is observed to be degraded by a factor of two. The resolutions on the other track parameters are affected by a factor three at most in the same scenario.

The global efficiency of the track reconstruction is significantly affected by the tracker misalignment if the alignment uncertainties are not taken into account in the track fit. The efficiency is fully recovered when the alignment uncertainties and the intrinsic position resolutions are combined to give the hit position error used in the track fit. In this case the fake rate increase from 3.5% up to 10% in the range of $1.5 < |\eta| < 2$.

The vertex reconstruction is affected by the tracker misalignment. The primary vertex efficiency drops 3.5% at most while the primary vertex position is degraded by 6-8 $\mu\mathrm{m}$ in x,y,z for the three physics channels studied.

X- and Y-coordinates				
	$\sigma_{x,y}$ [μm]	95% coverage [μm]	Bias [μm] X	Y
Perfect tracker alignment				
$B_s^0 \to J/\psi\phi$	45	119	-0.5 ± 0.6	-0.6 ± 0.6
$t\bar{t}H$	10	26	-0.0 ± 0.2	0.1 ± 0.2
DY	13.5	46	0.2 ± 0.3	-0.5 ± 0.3
Short-term tracker alignment				
$B_s^0 \to J/\psi\phi$	51	128	-5.8 ± 0.7	12 ± 0.7
$t\bar{t}H$	18	47	2.4 ± 0.2	16 ± 0.2
DY	24	62	1.6 ± 0.4	16 ± 0.4
Long-term tracker alignment				
$B_s^0 \to J/\psi\phi$	51	127	-10 ± 0.7	11 ± 0.7
$t\bar{t}H$	17	47	-9.5 ± 0.4	11 ± 0.4
DY	22	59	-8.9 ± 0.4	11 ± 0.4

Table 5: Primary vertex finding resolutions, fraction of tails, biases (x and y coordinates).

References

[1] *The Tracker Project TDR*, **CERN/LHCC 2000-016, CMS TDR 5 Addendum 1, 21 February 2000**.

[2] A. Ostapchouk *et al.*, *The Alignment System of the CMS Tracker*, **CMS Note 2001/053**.

[3] P. Vanlaer *et al.*, *Vertex reconstruction in CMS*, **CMS CR 2003/058**.

[4] R. Frühwirth, *Application of Kalman filtering to track and vertex fitting*, **Nucl. Instrum. and Methods. A 262 (1987) 444**.